Technical Report Number 443

August 1976

An Analysis of the Cooling of Intrusives by Ground Water Convection which Includes Boiling

L. M. Cathles

Ledgemont Laboratory
Kennecott Copper Corporation
Lexington, Massachusetts 02173

II. MATHEMATICAL FORMULATION AND METHOD OF SOLUTION

A. Physical and Mathematical Formulation*

For the fluid flow description we may begin with the Navier-Stokes equation:

$$\rho \frac{d\underline{v}}{dt} = - \underline{\nabla} p + \rho \underline{g}_o + \rho\nu\underline{\nabla}^2 \underline{v}$$

For flow through a porous media or fractured rock the Laplacian operator may be replaced by $-\zeta/d^2$, where ζ is a constant, d is the "effective" dimension of the pores or fractures, and the negative sign is required for the media to offer resistance to flow as it must physically. Neglecting inertial terms (i.e. assuming slow flow), the Navier-Stokes equation becomes:

$$- \underline{\nabla} p + \rho\underline{g}_o - \frac{\zeta\nu}{d^2} \rho\underline{v} = 0$$

If $\rho\underline{v}$ is replaced by the Darcy flux $\underline{q}$, where $\underline{q} = \rho\underline{v}\Phi_f$ and $\frac{d^2\Phi_f}{\zeta} \equiv k'$, the permeability of the formation in cm^2, we obtain Darcy's Law for flow in a porous or fractured media:

(1) $$- \underline{\nabla} p + \rho\underline{g}_o - \frac{\nu}{k'} \underline{q} = 0.$$ Momentum Balance

---

* All symbols are defined in Appendix I.

If joints were perfectly planar and regularly spaced, d would just be the aperature of the joints and ζ would have a value of 12, a result which can be obtained by solving the Navier-Stokes equation for flow between parallel plates and arranging the pairs of plates into a joint-like pattern (see for example Snow, 1968)**.

Equation (1) states that if $\underline{q} = 0$, p and ρ (call them p_o and ρ_o, indicating $\underline{q} = 0$) must be functions of z only. This is required because $\underline{g}_o = -g_o\hat{z}$.

$$(2) \qquad \underline{\nabla} p_o = -\rho_o g_o \hat{z} \quad \frac{\partial p_o}{\partial x} = \frac{\partial p_o}{\partial y} = 0 \text{ and } p_o = p_o(z)$$

$$p_o(z) = -\int_o^z \rho_o g_o dz \qquad \rho_o = \rho_o(z),$$

which is just the normal (no flow) increase in hydrostatic pressure with depth. Thus THERE CAN BE NO FLUID FLOW ($q = 0$) ONLY IF THE

** Unfortunately joints are not perfectly planar and the resistance they offer to flow is controlled by their irregularities (constriction) not their regularities (average aperature). Thus in practice it is not easy to estimate d, the "effective" fracture aperature so as to give a reliable estimate of permeability. The important point for us, however is that Darcy's Law applies to flow through fractures as well as to flow through the pores in a sandstone, a point which is underscored by the generality of the derivation (e.g. d can apply to pore diameter or fracture aperature).

Darcy's Law remains a valid description of flow through a porous or fractured media provided the Reynolds number (defined below) is less than $\sim$1.0 (Muskat, 1937, p.62; Elder, 1966, p.27).

$$R_m = \frac{qd}{\nu\rho} .$$

If we take the effective fracture aperature, d, to be less than .03cm (a restriction certainly appropriate for at least the porphyry copper environment where fractures are closely spaced and permeabilities low), since $\rho\nu$ is always greater than 10^{-4} (see Keenan et al, 1969, Table 7) $R_m < 1$, provided $q < 10^5$ g/cm^2-yr. The greatest flows we consider are $\sim$35 g/cm^2-yr.

FLUID DENSITY DOES NOT VARY LATERALLY. If ρ is a function of x or y the resulting buoyant forces will produce fluid flow*.

Heat balance is most easily deduced from physical reasoning. The increase in heat content of a volume of media (rock plus water) must equal the sum of the contribution of heat of reaction, fluid advection and conductive losses:

Increased heat content of volume of media	=	Heat sources within volume	+	fluid advection of heat into volume	+	net conductive transport into volume

$$\rho_m c_m \frac{\partial T}{\partial t} = A - \nabla \cdot \underline{q}\mathcal{H} + K_m \nabla^2 T \qquad (3)$$

Note we have assumed K_m is constant; this is a good approximation for the rocks we shall consider.

The fluid advection term is just the net heat carried into a volume element as a result of the fluid motion. For example:

---

* In the case of Rayleigh-Benard convection between two parallel surfaces across which a temperature differential is artificially maintained, conduction of heat in the fluid acts to smooth out horizontal temperature differences. A critical temperature differential must be exceeded before fluid motion can steadily maintain horizontal temperature differences against this conduction. In the case of an intruding pluton, horizontal temperature differences will be maintained automatically at the edges of the pluton. Thus ground water convection will automatically occur, no critical temperature difference need be exceeded, and we deal to some extent at least with a case of forced rather than free convection. The nature of the convection (forced or free) does not affect the mathematical formulation and is determined solely by the boundary and initial conditions chosen.

(3a) $$-\nabla \cdot (q_x \mathcal{H} \hat{x}) = \{(q_x \mathcal{H})^- \Delta z \Delta y - (q_x \mathcal{H})^+ \Delta x \Delta y\} / \Delta x \Delta y \Delta z$$

$$= \{\text{Heat carried in by fluid flow - heat carried out by fluid flow}\}/\text{volume.}$$

Conservation of fluid mass* requires:

(4) $$\nabla \cdot \underline{q} = 0. \quad \text{Mass Balance}$$

It is assumed in (3) that fluid and rock are everywhere at the same temperature. The validity of this assumption depends upon the rate at which the temperature of the system changes and upon the spacing of the fractures or joints through which hydrothermal solutions flow. In the cases we consider changes in temperature are not great over periods of time of 100 years or so ($<20^oC$). The interiors of the "matrix blocks" between fractures will be able to track these changes in fracture temperature so as to remain essentially isothermal provided the fractures are less than a few hundred meters apart**. In the models presented in this study

---

* i.e. the continuity equation $\frac{\partial \rho}{\partial t} + \nabla \cdot (\rho \underline{V}) = 0$ requires $\nabla \cdot \underline{q} = 0$ if $\frac{\partial \rho}{\partial t} = 0$. In the older literature it is commonly assumed $\nabla \cdot \underline{V} = 0$ which implicitly assumes $\rho \cong$ const. This is not an appropriate condition when the system is hot enough to be near boiling and where substantial fluid density changes from one location to another must be expected.

** For example a sphere of diameter D (equal to the joint or fracture spacing), initially at 100^oC, will take the following times to cool so that its central temperature is 4^oC if its surface is suddenly fixed at 0^oC at $t = 0$:

D =	10 cm	100 cm	10 m	100 m	500 m	1000
t_{4^oC} =	15 min	1 day	.28 yrs	28 yrs	723 yrs	2790 yrs

(Carslaw and Jaeger, p.234; conductivity, rock density, and heat capacity as in Appendix I). Thus a matrix block 100 m on a side will have little trouble following changes in temperature of fluids flowing along its sides, provided the temperature of the fluids change reasonably slowly over time scales of 100 years or so.

it is therefore implicitly assumed "flow" fractures (or joints) are less than 200 m apart. This assumption is implicit because it is not necessary to explicitly conceptualize the mode of flow through the formation (which is described by an "average" permeability). It is only necessary to make sure the likely mode of fracture flow will not violate assumptions made elsewhere (such as in temperature calculations)

Heat sources within a rock volume may be of two types: (a) Heats of crystallization (as the melt portion of an intruding pluton cools) or (b) Heats from exothermic chemical reactions (which occur as convecting fluids interact with and cool the intruding pluton). Both of these internal sources of heat may be substantial, being ∿50 cal/g of rock (Norton and Cathles; Fyfe, 1974) or about 12% of the heat stored due to the heat capacity and elevated temperature of a 700°C intruding pluton.

In this paper we consider fluid interaction with a pluton after it has cooled sufficiently to develop through-going fractures. Internal sources of heat due to crystallization are ignored in our treatment. Lister (1974) has considered how such through-going fractures may develop.

It is convenient to express heat sources due to chemical reactions:

$$A_R = -R\rho_m \frac{\partial T}{\partial t} \tag{5}$$

R is the average heat of reaction over 600°C of cooling and is taken to have a value of 36/600 = .06 cal/g - °C. R could be given a temperature dependence to more closely track the heats of reactions taking place at various temperatures (see Carnahan et al, 1969, p.464). We take R constant for the purposes of calculations presented here.

Taking (5) into account the heat balance equation (3), becomes:

(6) $$(R + c_m)\ \rho_m \frac{\partial T}{\partial t} = - \underline{\nabla} \cdot \mathcal{H}\underline{q} + K_m \nabla^2 T$$ Energy Balance

Equations (1), (4) and (6), together with boundary and initial conditions, which are discussed later, describe what will happen when a hot igneous pluton intrudes water saturated rock of permeability k'.

For the purposes of numerical modeling it is convenient to put (1) in the form of a second order elliptic partial differential equation similar to (6). This may be done by using Helmholtz's theorem which states that any vector field can be expressed as the sum of the gradient of a scalar field and the curl of a vector field:

$$\underline{q} = - \underline{\nabla}\Phi + \underline{\nabla} \times \underline{\psi}$$

Equation (4) allows the above equation to be simplified since it indicates $\nabla^2\Phi = 0$; ($\underline{\nabla} \cdot \underline{\nabla} \times \underline{\psi} \equiv 0$). Thus if $\underline{q}$ is zero far away from the region of interest (i.e. there is no regional ground water flow), $\nabla\Phi = 0$ on the boundary of the solution domain, or Φ = constant. Since there are no sources of Φ inside the domain (Φ satisfies Laplace's equation), Φ is constant everywhere and we may without further loss of generality take $\Phi = 0$. Therefore:

(7) $$\underline{q} = \underline{\nabla} \times \underline{\psi} ,$$

or in the two dimensional problems we consider:

(7a) $$q_z = \frac{-\partial \psi_x}{\partial y}$$

$$q_y = \frac{\partial \psi_x}{\partial z}$$

Also since $\underline{\nabla} \times \underline{\nabla} \cdot \underline{\psi} = 0$, we may discard the divergent part of $\underline{\psi}$ and assume $\underline{\nabla} \cdot \underline{\psi} = 0$ without loss of generality.

If (7) is now substituted into (1), and the curl of (1) taken, using $\underline{\nabla} \cdot \underline{\psi} = 0$:

$$(8) \qquad \frac{\nu}{k'} \nabla^2 \underline{\psi} - \underline{\nabla} \left(\frac{\nu}{k'}\right) \times \underline{\nabla} \times \underline{\psi} + g_o \underline{\nabla} \times \rho \hat{z} = 0.$$

It is conventional to make equations (5) and (8) dimensionless by substituting:

x	$=$	$\bar{x}H$	H	$=$	depth extent of system
ν	$=$	$\bar{\nu}\,\nu^*$	ν^*	$=$	$.01\ cm^2/sec$
k'	$=$	$\bar{k}'k'^*$	k'^*	$=$	$10^{-11}\ cm^2$ = 1 millidarcy
T	$=$	$\bar{T}\,T^*$	T^*	$=$	$1^oC.$
ρ	$=$	$\bar{\rho}\,\rho^*$	ρ^*	$=$	$1.0\ g/cm^3$
$\mathcal{H}$	$=$	$\bar{\mathcal{H}}\mathcal{H}^*$	$\mathcal{H}^*$	$=$	1 cal/g

$$(9) \qquad \underline{g} = -g_o \hat{z}$$

$$t = \bar{t}\ \frac{\rho_m c_m H^2}{K_m}$$

$$p = \bar{p}\ \frac{K_m \nu^*}{\mathcal{H}^* k^*}$$

$$\underline{q} = \underline{\bar{q}}\ \frac{K_m T^*}{H \mathcal{H}^*}$$

$$\underline{\psi} = \underline{\bar{\psi}}\ \frac{K_m T^*}{\mathcal{H}^*}$$

$$\underline{\nabla} = \underline{\bar{\nabla}}/H$$

A star (*) indicates a constant quantity that is generally chosen to be typical or appropriate to the problem at hand. For example k'^* might be the average permeability of the permeability at some particular location, ν^* a typical kinematic viscosity, etc. If (9) is used and if $\underline{\psi} = \psi_x(y,x)\,\hat{x}$ (i.e. we consider two dimensional problems), (6) and (8) become:

(10a) $$0 = \frac{\bar{k}'}{\bar{\nu}}\ \bar{\nabla}\cdot\left(\frac{\bar{\nu}}{\bar{k}'}\ \bar{\nabla}\ \bar{\psi}_x\right) - \frac{\mathcal{H}^* g_o k'^*\ \rho^* H}{T^*\ \nu^* K_m}\ \frac{\bar{k}'}{\bar{\nu}}\ \frac{\partial\bar{\rho}}{\partial\bar{y}}$$

(10b) $$\left(1 + \frac{R}{c_m}\right)\frac{\partial\bar{T}}{\partial\bar{t}} = \bar{\nabla}^2\bar{T} - \bar{\nabla}\cdot\bar{q}\,\bar{\mathcal{H}}$$

Once the flow has been determined from the solutions of (10a, b), the pressure anywhere can be determined from the integrated form of (1):

$$p(z) = p_s + g_o\int_z^s \rho(z)\,dz + \int_z^s \frac{\nu(z)}{k'(z)}\,q_z(z)\,dz$$

or in terms of the dimensionless quantities of (10a, b),

(11) $$p(z) = p_s + g_o\rho^* H\int_{\bar{z}}^{\bar{s}} \bar{\rho}(z)\,d\bar{z} + \frac{\nu^* K_m T^*}{k'^*\mathcal{H}^*}\int_{\bar{z}}^{\bar{s}} \frac{\bar{\nu}}{\bar{k}'}\,\bar{q}\,d\bar{z}\ .$$

$\bar{s}$ is the "surface".

Equation (11) gives the relative pressure everywhere as a vertical column. The pressure at a single point in that column, p_s, then specifies the absolute pressure. Here we assume the pressure at the surface (s) is known. We could as well assume the pressure at some depth was unperturbed and thus known. As discussed later this assumption may be preferable in many cases, and the pressure contours plotted in the figures assuming p_s = 10 Bars therefore require some interpretation.

With the temperature known everywhere from the solution of (10b) and pressure known everywhere from the solution of (10a) and (11), suitable values of $\rho(T,p)$, $\nu(T,p)$, and $\mathcal{H}(T,p)$ can be looked up in tables appropriate for pure water. Thus the true properties of water can be taken into account in the calculation of convection, as discussed further in the next section.

Equations (10) are more general than those generally quoted in the literature. $\overline{\nu}$, $\overline{\mathcal{H}}$, and $\overline{\rho}$ can have any variation with temperature and pressure. If $\overline{\rho}$ is approximated and $\overline{\rho} = 1 - \alpha T$, and $\mathcal{H} = c_f T$, and k', ν, α, c_f are assumed constant, and R = 0, equation 10a, b become:

(13a) $$0 = \overline{\nabla}^2 \overline{\psi}_x + \mathcal{R}_T \frac{\partial \overline{T}}{\partial \overline{y}}$$

(13b) $$\frac{\partial \overline{T}}{\partial \overline{t}} = \overline{\nabla}^2 \overline{T} - \overline{\underline{q}} \cdot \overline{\nabla}\, \overline{T}$$

$$\mathcal{R}_T = \frac{c_f^* g_o k'^* \rho^* H T^* \alpha}{\nu^* K_m}$$

$\mathcal{R}_T$ is the thermal Rayleigh number; T* in $\mathcal{R}_T$ is usually taken to be the maximum temperature difference in the system, not 1^oC as in (9).

Equations (13) are equivalent to equations given by Holst and Aziz (1972) and Donaldson (1962, 1968). These authors assume $\underline{\nabla} \cdot \underline{q} = 0$ as we do here. Under the above restrictions equations (13a, b) are also quite similar to equations given by Palm et al (1972), Elder (1967), Lapwood (1948), and Rubin (1973), who assumed $\nabla \cdot V = 0$ and therefore that $\rho = \text{const}$.

B. Method of Solution

Equations 10a, b are of the form or may be put in the form:

$$E \frac{\partial T}{\partial t} = \frac{1}{F} \underline{\nabla} \cdot F \underline{\nabla} T - \underline{\nabla} \cdot \underline{q} \gamma T + Q \tag{14}$$

E, F, T, q, γ, and Q may all be functions of both y and z. γ has been introduced assuming $\gamma T = \mathcal{H}$. This definition will be discussed later. (14) may be solved by finite different techniques. The approach used was to write a subroutine to solve (14) subject to arbitrary boundary conditions.

$$AT + B \frac{\partial T}{\partial n} = G \tag{15}$$

$\frac{\partial T}{\partial n}$ represents the derivative of T normal to the boundary. A, B, and G may be functions of position along the boundary so, for example, at one point T might be specified to equal $20^{\circ}C$ by setting B, G = 20, A = 1, while at another point the heat flux might be set equal to zero by specifying A, G = 0, B = 1 (so that $\partial T/\partial n = 0$). For free flow condition A = 0, B = 1, G = 0; for no flow boundary condition A = 1, B = 0, G = 0.

The solution of (14) subject to (15) was achieved using the standard ADI (Alternating Direction Implicit) method described by Carnahan et al (1969 p.452ff). The routines were written so that the grid spacing could be varied in any specified manner in either

the y or the z directions*. A typical grid is shown in Figure 1. When a steady state solution was desired (as in the fluid flow case) the rapid convergence scheme of Peaceman and Rachford (1955) was used.

A variable spacing is necessary to compute reliable surface heat fluxes for "no flow" top surface boundary conditions. It is important to have the first line of points near the surface if the possibility of high surface heat flux is to be accommodated. At the same time computation cost would be unduly great if this close surface point spacing were achieved by taking a large number of points (i.e. having a close grid spacing at depth where it is not really needed). The solution is to have a variable grid spacing with close spacing near the surface.

An indication of the importance of this procedure may be illustrated as follows: A uniform flow grid with 19 points would have a first line of points 277 m below the surface. When no flow out the top is allowed the temperature anomaly has always cooled to $\sim 200^{\circ}C$ by the time the near surface is reached and vertical near surface flow is small. With uniform spacing the maximum heat flux we could expect, therefore, would be

$$HF = (10^6)(6 \times 10^{-3} \text{cal/cm}^2\text{-}^{\circ}\text{C-sec})\left(\frac{200^{\circ}C}{277 \times 10^2}\right) = 43 \text{ HFU.}$$

On the other hand with a variable grid spacing (N = 19) the first line of points is only 57.5 m below the surface and a heat flow of 208 HFU will be produced by a $200^{\circ}C$ temperature difference across

*i.e.

$$\frac{1}{F}\frac{\partial}{\partial z}\left(F\frac{\partial T}{\partial z}\right) = \left(\frac{F_{z+} + F_{zo}}{2F_{zo}}\,\frac{T_{z+} - T_{zo}}{(\Delta z_+ + \Delta z_o)/2} - \frac{F_{z-} + F_{zo}}{2F_{zo}}\,\frac{T_{zo} - T_{z-}}{(\Delta z_o + \Delta z_-)/2}\right) \Big/ \{(\Delta z_o + (\Delta z_+ + \Delta z_-)/2)/2\}$$

Figure 1: Diagram of solution domain for conductive and k' = .05 md cases. Dots indicate the points at which finite difference approximations to the solution are computed. Point spacing is variable in both the $\hat{y}$ and z directions. The intrusive was taken to occupy the first 6 $\hat{z}$ points and the first 5 $\hat{y}$ points as shown. Boundary conditions for temperature and fluid flow were taken as shown. The thermal balance solution is determined on a 16 by 20 grid with the top surface (I = 17) a boundary plane. Fluid flow is determined on a 15 by 18 grid with all sides boundary planes (no flow). In this way the solution domain for fluid flow and heat balance are coincident. The small derivation from coincidence when free flow out the top is permitted is not significant to the results of the calculations. The first line of points is 84.5 m beneath the surface.

For cases computed with k' > .05 md a 19 x 29 flow grid was used with variable spacing from the top and around the pluton edge. The depth to the first line of points in this case was 57.5 m. As commented in the text it is important to have the first line of points reasonably near the surface if surface heat fluxes are to be reasonably accounted for.

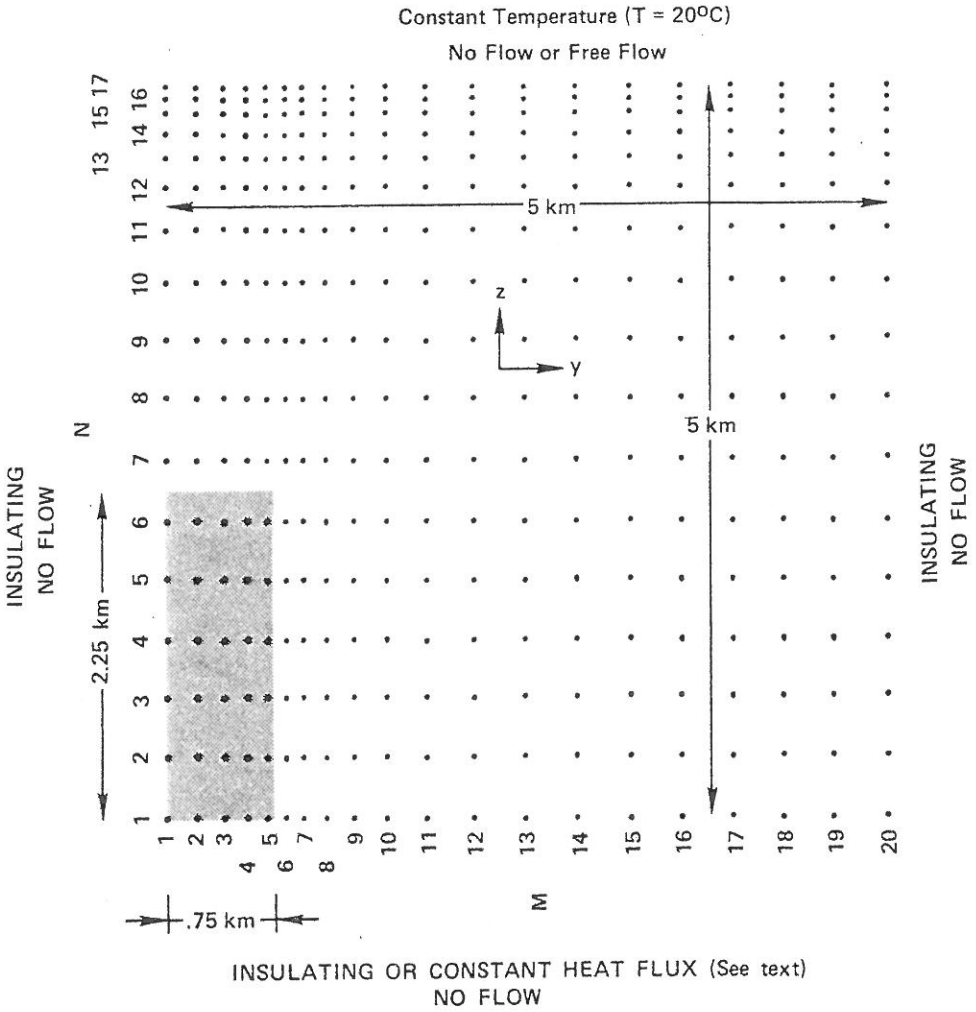
Constant Temperature (T = 20°C)
No Flow or Free Flow
5 km
z
y
5 km
INSULATING
NO FLOW
INSULATING
NO FLOW
2.25 km
.75 km
N
M
INSULATING OR CONSTANT HEAT FLUX (See text)
NO FLOW

Figure 1

this distance. A denser grid that could provide the same accuracy (87 points) would require at least 5 times longer to compute (assuming the horizontal grid remained unchanged).

Generally a constant heat flux of 1.5 HFU was assumed in the base of the solution domain and a surface temperature of 20°C was assumed. An increase in temperature with depth consistent with these boundary conditions (and $K_m = 6 \times 10^{-3}$ cal/cm^2-sec-°C) was taken for an initial temperature distribution. Into this normal geothermal gradient a 700°C pluton of specified geometry, was suddenly intruded at t = 0. The computations indicate how the pluton cools through the agencies of conduction and convection.

The basal boundary condition of constant heat flux was modified somewhat in the neighborhood of the pluton to avoid the base of the pluton heating up above its intrusion temperature. If the temperature at the base was greater than indicated by the normal geothermal gradient, the heat flux into the base was set equal to zero.

Since heat flux out the top will continue at near the normal 1.5 HFU (or more if the thermal anomaly has reached the surface), changing the basal boundary condition in this way has the effect of allowing the system to lose heat. In nature a pluton might lose some heat downward as well as upward to the surface. The heat lost downward (by conduction) would cause anomalous heating of the substrate. This energy would eventually migrate to the surface, causing a long term, weak heat flow anomaly. We allow for the downward loss of heat but do not store the heat in a substrate and so neglect these long term effects on heat flow. The problem of downward diffusion of heat can be reduced by taking the pluton in the middle of a larger solution domain as is done in some of the cases presented later.

Equations (10) were solved cyclically as shown in Figure 2. From the starting values, the temperature distribution a short time later was calculated by using the primary subroutine and (10b). From the temperature distribution the fluid flow was calculated using (10a). Values of the pressure everywhere in the solution domain (at the end of the timestep) were calculated using (11) and P_s = 10 bars, and values of $\bar{\nu}$, $\bar{\rho}$, and $\bar{\mathcal{H}}$ at the end of the timestep were looked up from p-T tables (see Figures 3a-3c). Linear extrapolation was used between table entries. The average of $\bar{\nu}$, $\bar{\rho}$, $\bar{\mathcal{H}}$ at the beginning and end of the timestep and the fluid flow at the end of the timestep were then used to calculate a more accurate temperature at the end of the timestep. The solution so obtained was output and the solution for the next time step computed in the same fashion. This is the standard method of solving coupled non-linear equations (i.e. see Elder, 1967; Donaldson, 1962; Holst and Aziz, 1972). The only difference is the true properties of water are taken into account using tables and the advection term is given improved treatment, as discussed below, that can account for fluid boiling and condensation.

Stability problems in finite difference computations of this sort originate almost entirely in the non-linear advection term, $\underline{\nabla} \cdot \underline{q}_\gamma T$. This term was computed implicitly using a method which takes into account the direction of fluid convection so that it computes upstream gradients only and thus preserves causality (upstream anomalies are "advected" downstream; anomalies do not swim upstream). The method used is discussed in detail by Torrance (1968, Method V of Table 1). Some false diffusion is produced but this disadvantage appears minor and is outweighed by the stability of the method and the fact that the method is conservative and physically sensible.

Figure 2: Flow chart for calculation of the convective cooling of an igneous intrusion suddenly intruded at some specified temperature into a water saturated permeable formation.

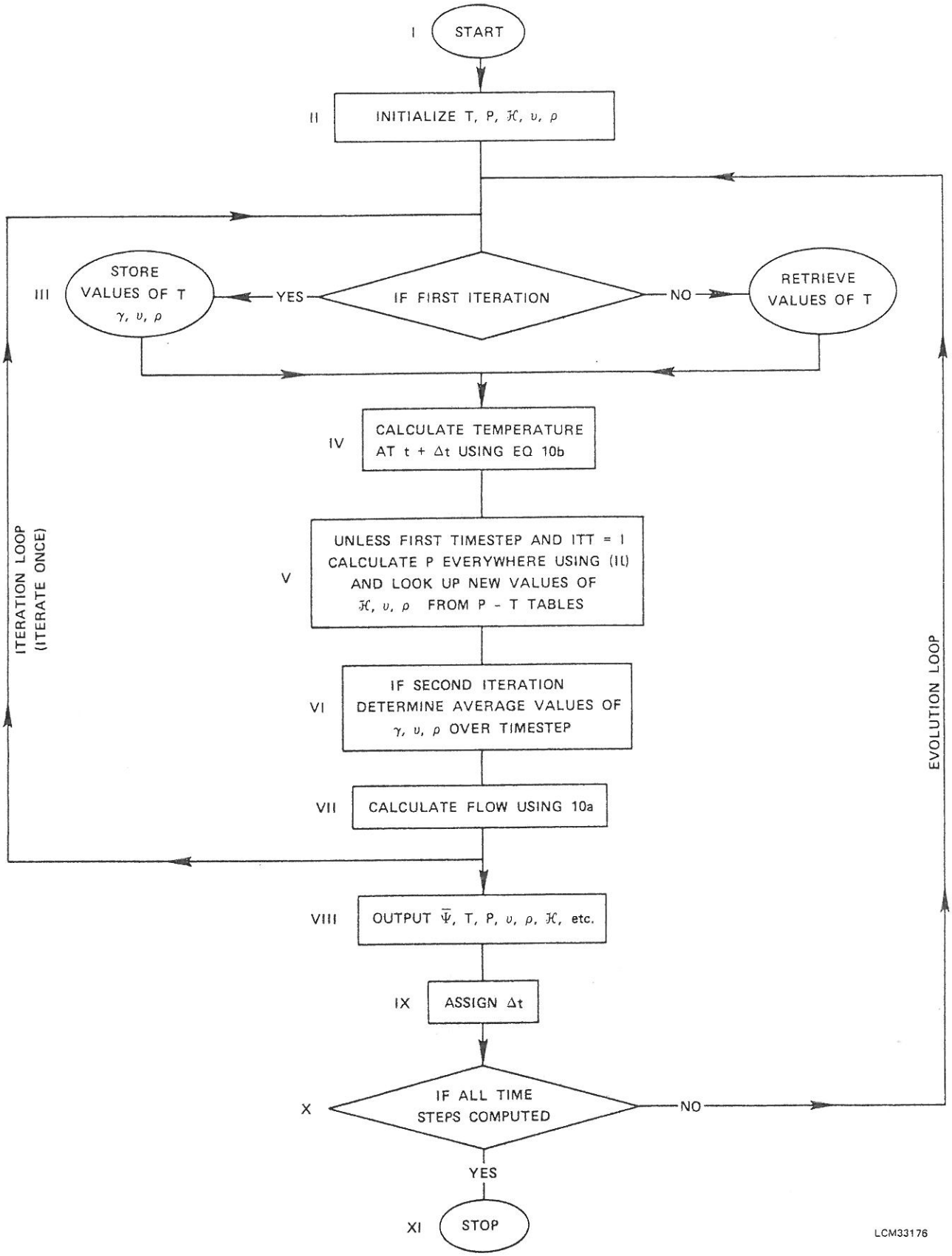
I START
II INITIALIZE T, P, $\mathcal{H}$, υ, ρ
III STORE VALUES OF T γ, υ, ρ
YES
IF FIRST ITERATION
NO
RETRIEVE VALUES OF T
IV CALCULATE TEMPERATURE AT t + Δt USING EQ 10b
V UNLESS FIRST TIMESTEP AND ITT = 1 CALCULATE P EVERYWHERE USING (II) AND LOOK UP NEW VALUES OF $\mathcal{H}$, υ, ρ FROM P - T TABLES
VI IF SECOND ITERATION DETERMINE AVERAGE VALUES OF γ, υ, ρ OVER TIMESTEP
VII CALCULATE FLOW USING 10a
VIII OUTPUT $\bar{\Psi}$, T, P, υ, ρ, $\mathcal{H}$, etc.
IX ASSIGN Δt
X IF ALL TIME STEPS COMPUTED
NO
YES
XI STOP
ITERATION LOOP (ITERATE ONCE)
EVOLUTION LOOP
LCM33176

Figure 2

γ (in the advection term) is initially defined at each grid point as $\mathcal{H}'T'$, where $\mathcal{H}'$ and T' are the values of enthalpy and temperature at the grid point during the previous time step. Taking $\gamma = 1$ would be equivalent to assuming a constant heat capacity of 1 cal/gm, an approximation which could be over 100% incorrect (see Figure 3b). This definition of γ introduces some instability at high formation permeabilities because the γ of the previous time step is not strictly appropriate for the time step of the computation. This error can be minimized by taking small time steps and by averaging old and new estimates of γ in the iteration loop.

Boiling is automatically taken into account by the procedures followed. How the method of computation takes into account the heats of vaporization and condensation is best understood with reference to Figure 3b and equation (3a). Suppose a packet of water is convecting upward across the critical curve in the region where γ would go from near 2 to near 1 cal/gm-^{o}C. This crossing would occur near 300^{o}C and 100 bars. Remembering that $\mathcal{H} \equiv \gamma T$, and T must be continuous across small distances, we see from (3) that the advection term, $-\underline{\nabla} \cdot \underline{q}\mathcal{H}$, equals $(\gamma^{-} - \gamma^{+})\, qT\, \frac{\Delta x \Delta y}{\Delta x \Delta y \Delta z}$. Since $\gamma^{-} - \gamma^{+} \cong 1$ cal/gm = ^{o}C, we see the advection term accounts for a latent heat of condensation of $\sim$300 cal/gm. The mass flux into the area $\Delta x \Delta y$ is q gm/cm^{2}, and the volume heated by the resulting release of latent heat is $\Delta x \Delta y \Delta z$.

Thus we see the advection term, together with the data shown in Figure 3b, automatically accounts for the latent heats of vaporization and condensation. The direction of fluid motion is known to the advection term so condensation is automatically distinguished from vaporization.

The normal component of q is of course continuous across the boiling boundary (the amount of water convecting up to the boundary cannot exceed the amount of steam leaving). It is assumed that the boundary between gas and liquid is sharp, that liquid converts immediately to gas and vice versa. This is equivalent to assuming

p-T variations along a streamline do not follow the critical curve of water (along which liquid and gas can coexist) for any appreciable distance. The results of computations show that in general the streamline p-T curves intersect the critical curve of water at high angles (see Figure 9). Thus the critical curve is crossed cleanly and the assumption of a sharp boundary between gas and liquid is appropriate.

C. Accuracy

The method used in handling the non-linear advection terms in the heat flow equation is stable for all mesh sizes provided that the timesteps chosen are small enough. It need only be shown that the solution obtained converge by decreasing the mesh size and showing the solutions do not change significantly (Torrance, 1968). Since the convection equation contains no non-linear "advection" term there is no problem with its convergence.

Because of the non-standard treatment of enthalpy it was also verified that thermal energy was conserved with time.

The mesh sizes used in the computation presented in Section III are characterized by parameters given in Table 1. The vertical spacing was increased exponentially from a minimum value at $j = N$: $\Delta z_{j-1} = (\Delta z_j)$ (EXZ). This was done for the first NAL points from the top surface (See Fig. 1). The horizontal spacing was increased to the left and the right of the pluton edge, the point spacing on either side of the edge being equal. Thus to the right (see Fig. 1) $\Delta y_{j+1} = (\Delta y_j)$ (EXY); to the left $\Delta y_{j-1} = (\Delta y_j)$ (EXZ). To the right this increase in point spacing was continued for MAL points (including the first one). To the left it was continued to the boundary.

N	M	ΔZ_{min}[m]	ΔY_{min}[m]	ΔZ_{max}[m]	ΔY_{max}[m]	EXZ	NAL	EXY	MAL	PLUTON	Time List	Cases
16	20	85	120	408	359	1.3	7	1.2	7	i=1-6 j=1-5	#1	Fig.1,Fig.5a,b
19	29	62	90	561	366	1.3185	9	1.1916	9	i=6-9 j=1-6	#2	Fig.14a-c
19	29	58	77	346	237	1.2925	8	1.1515	9	i=1-7 j=1-7	#2	Fig.5c,6a,b,c Fig.12,13
29	29	35	77	214	237	1.22	10	1.1515	9	i=1-11 j=1-7	#3	Fig.4
39	29	25	77	155	237	1.18	12	1.1515	9	i=1-15 j=1-7	#3	Fig.4,(6a)

Time List #1 Δt = 25*.2, 2*.25, 2*.3, .4, 5*.5, 4*1., 2*2., 3., 6*5., 5*10.

#2 Δt = 25*.2, 2*.25, 2*.3, .4, 5*.5, 4*1., 2*2., 3., 16*5.

#3 Δt = 25*.2, 40*.25, 10*.5

Table 1: Parameters describing grid spacing and time increments for cases presented in Section III (see Figure 1, which illustrates the N=16, M=20 case, and discussion in text). ΔZ_{min} is the minimum vertical point spacing (at the top surface); ΔY_{min} is the minimum horizontal point spacing (at the pluton edge). ΔZ_{max} is the maximum vertical point spacing (at the base of the solution domain); ΔY_{max} is the maximum horizontal point spacing (at the right of the solution domain). "PLUTON" gives the points occupied by the pluton. EXZ, NAL, EXY, MAL are defined in the text. Plutons wider than .75 km half width had appropriately changed ΔY spacings.

Ledgemont Laboratory 128 Spring Street Lexington, Massachusetts